

Sensor Sampling Trade-Offs for Air Quality Monitoring With Low-Cost Sensors

Pau Ferrer-Cid, Julio Garcia-Calvete, Aina Main-Nadal, Zhe Ye, Jose M. Barcelo-Ordinas, Jorge Garcia-Vidal

Abstract—The calibration of low-cost sensors using machine learning techniques is a methodology widely used nowadays. Although many challenges remain to be solved in the deployment of low-cost sensors for air quality monitoring, low-cost sensors have been shown to be useful in conjunction with high-precision instrumentation. Thus, most research is focused on the application of different calibration techniques using machine learning. Nevertheless, the successful application of these models depends on the quality of the data obtained by the sensors, and very little attention has been paid to the whole data gathering process, from sensor sampling and data pre-processing, to the calibration of the sensor itself. In this article, we show the main sensor sampling parameters, with their corresponding impact on the quality of the resulting machine learning-based sensor calibration and their impact on energy consumption, thus showing the existing trade-offs. Finally, the results on an experimental node show the impact of the data sampling strategy in the calibration of tropospheric ozone, nitrogen dioxide and nitrogen monoxide low-cost sensors. Specifically, we show how a sampling strategy that minimizes the duty cycle of the sensing subsystem can reduce power consumption while maintaining data quality.

Index Terms—Air Quality, Low-Cost Sensors, Sampling, Sensor Calibration, Machine Learning

I. INTRODUCTION

IN recent years, much effort has been devoted to investigating energy-saving mechanisms in the design of wireless sensor networks. Most of this effort has focused on the communications subsystem [1], and one of the most successful techniques has been the design of media access protocols that optimize the duty cycle, taking advantage of the fact that the states through which the radio chipset passes have different energy consumption. However, little attention has been paid to the energy consumption of the sensing subsystem, assuming most of the time that sampling is done instantaneously and at a negligible energy cost. The major efforts made regarding the reduction of energy consumption in the sensing subsystem are in in-network aggregation techniques, in which the aggregation process is performed in the multi-hop network [2]. The case of low-cost air pollution sensors is a different scenario. These sensors report hourly data that are the result of the aggregation of the samples taken during that hour in the sensor subsystem

Pau Ferrer-Cid (pau.ferrer.cid@upc.edu), Aina Main-Nadal (aina.main@est.fib.upc.edu), Zhe Ye (zhe.ye@estudiantat.upc.edu), Jose M. Barcelo-Ordinas (jose.maria.barcelo@upc.edu) and Jorge Garcia-Vidal (jorge.garcia@upc.edu) are with the Universitat Politècnica de Catalunya, Barcelona, Spain. Julio Garcia-Calvete (julio468@gmail.com).

This work is supported by the National Spanish funding PID2019-107910RB-I00, by regional project 2017SGR-990, and with the support of Secretaria d'Universitats i Recerca de la Generalitat de Catalunya i del Fons Social Europeu.

of each node. The way these samples are taken and the aggregation strategy have a great impact on the energy consumption of the sensor subsystem.

An additional challenge of these sensor networks that measure air pollution is that since the sensors have not been calibrated by the manufacturer or, they have been calibrated in laboratory chambers, they need to be calibrated in the environmental conditions of the deployment site [3], [4]. Just as the sampling, pre-processing and aggregation tasks are performed at the sensing node (edge computing), the calibration task is performed off-line in the cloud. There, depending on the calibration method, a set of coefficients or hyperparameters are obtained that then allow predicting the calibrated data from the raw samples taken by the sensors. This way of calibrating sensors is called calibration in uncontrolled environments [3]. These calibration techniques are based on linear or nonlinear supervised machine learning mechanisms, such as multiple linear regression (MLR) [5], [6], k-nearest neighbors (KNN) [5], random forests (RF) [5], [7], [8], support vector regression (SVR) [5] and artificial neural networks (ANN) [6], [9] among others.

To calibrate air pollution sensors in an uncontrolled environment, they must be placed next to reference instrumentation, and therefore with the same sampling frequency as that used by the reference instrumentation. This methodology is known as *in-situ* calibration [3], [4]. A widely used technique for these sensors is to use government reference stations [10], [11] which, when connected to an uninterruptible power supply, aggregate the samples and display them every T_{ref} ¹ [5], [7], [8], [12]–[18]. Low-cost sensors can follow a similar strategy if they are continuously powered, taking high-frequency samples² and aggregating them into the same reference data periodicity T_{ref} . However, if the nodes are powered by batteries it is challenging to implement a duty cycle-based strategy. The reason is that many of these sensors have a response period that can be on the order of several minutes before a correct measurement can be made, and also different air pollution phenomena may require different data sampling frequencies.

The objective of this work is to analyze effective sampling strategies in this type of air quality sensor networks, where it is necessary to implement a duty cycle strategy that saves

¹For example, reference stations that display O_3 , NO_2 or PM_x in Europe take samples continuously, during at least 45 minutes every hour, and display them every hour, see European directive 2008/50/EC.

²In the air pollution monitoring field, where reference stations provide measurements every hour, 2.7×10^{-4} Hz, a sampling period of few seconds is considered high frequency.

energy in the sensor subsystem while achieving the best quality of reported data, according to the chosen calibration method. We place special emphasis on the impact that sensor sampling strategy has on calibration quality, as well as the impact of the resulting duty cycle. To this end, we calibrate the O_3 , NO_2 and NO electrochemical sensors with the best subset of sensors for calibration using different duty cycle strategies. The experiments are performed using data collected by an experimental internet of things (IoT) node called Captor, which measures O_3 , NO_2 , NO , temperature and relative humidity, and whose hardware and software have been developed to sample intensively in order to be able to simulate several sampling strategies. Specifically, in this work we:

- describe the prototype node used to simulate the duty cycle strategies,
- perform a feature selection to show the best subset of sensors to be included in the sensor calibration,
- perform a multiple linear regression calibration of O_3 , NO_2 and NO sensors, assuming high data availability,
- simulate different sensor sampling strategies, showing their impact on the goodness-of-fit of the calibration, as well as the implications of the resulting duty cycles.

The different sections are organized as follows: section II shows the related work. Section III describes the experimental node used in this research work. Then, section IV introduces the different pre-processing steps required for sensor calibration. Section V shows the different experiments performed. Finally, section VI presents the conclusions of the paper.

II. RELATED WORK

Low-cost sensors in air pollution: the use of low-cost sensors for air pollution monitoring has been the subject of study during the last few years [11], [19], [20]. These sensors provide a cost-effective alternative to complement measurements from high-cost government-deployed instrumentation. The low cost of these sensors leads to low data quality, therefore the calibration of low cost sensors has been studied in depth during the last years in order to improve the quality of the data [3], [8], [16], [21]. Studies have been carried out to verify whether low-cost sensors can obtain accurate measurements and whether they can be included in a regulated way for air quality monitoring [9], [11], [22]. Motlagh *et al.* [23] suggest that the future of air pollution monitoring networks lies in the creation of heterogeneous networks composed of hundreds of low-cost sensors and high-precision instrumentation.

Low-cost sensor calibration: the most widely used technique for improving the quality of low-cost sensor data has been *in-situ* calibration using machine learning techniques [16], [24], [25]. *In-situ* calibration consists of placing the sensor in a reference station and using the obtained sensor values and reference values to train a supervised machine learning model [4]. There are several studies that use multiple linear regression (MLR) to calibrate sensors of different gases [18], [26]. These methods have been shown to be very effective in improving data quality. Furthermore, nonlinear machine learning techniques, which are able to better adapt to the nonlinearities present in these sensors, have also been applied

[9], [18]. In particular, techniques such as k-nearest neighbors (KNN) [5], random forests (RF) [7], [25], Gaussian processes (GP) [14], support vector regression (SVR) [5] and artificial neural networks (ANN) [9], [18] have been used. Different air pollutants are known to have cross-correlations with other pollutants, as well as some sensors have cross-sensitivities with other pollutants for which they have not been designed [9], [27]. Hence, the sensors to be introduced in the calibration is another key point of the application of these machine learning techniques, so that the calibration benefits from cross-sensitivities and cross-correlation. This way, selecting the best array of sensors is commonly known as feature selection in the machine learning paradigm. As an example, Mijling *et al.* [13] show that the NO_2 sensor calibration benefits from the introduction of O_3 (O_3 can be a good NO_2 proxy) and temperature sensor measurements.

TABLE I
SENSOR SAMPLING PERIODS USED IN THE LITERATURE.

Work	Pollutants	Sampling Period (T_s)
Wang <i>et al.</i> [8]	PM _{2.5}	10 min
Mijling <i>et al.</i> [13]	NO ₂	1 min
Ferrer-Cid <i>et al.</i> [5]	O ₃	1 min
Nowack <i>et al.</i> [14]	NO ₂ , PM ₁₀	30 s
Bigi <i>et al.</i> [7]	NO, NO ₂	20 s
De Vito <i>et al.</i> [15]	NO ₂ , O ₃ , NO	20 s
Si <i>et al.</i> [16]	PM _{2.5}	6 s
Mead <i>et al.</i> [17]	NO	5 s
Han <i>et al.</i> [18]	O ₃ , NO ₂ , CO, SO ₂	2 s
Mead <i>et al.</i> [17]	CO, NO ₂	1 s
Astudillo <i>et al.</i> [21]	O ₃ , CO	1 s

Data aggregation in wireless sensor networks: there is a rich literature related to data aggregation and reduction of energy consumption in wireless sensor networks. Most of this literature is based on the idea of reducing power consumption³ in the communication subsystem by designing protocols that aggregate data along the path from the sensor to the sink, thus minimizing the number of packets to be transmitted in the network [1], [2]. The problem of data aggregation in air pollution sensor networks is different. The nodes are calibrated individually, and the aggregation is done in the node's sensing subsystem and not in the network, so the objective here is not to minimize the number of packets to be transmitted together in the network, but the energy consumption of the sensing subsystem while maintaining the quality of the calibrated data. This implies defining correctly how often the sensors' signal is sampled to maintain good data quality. Table I shows works in which the authors sampled at different frequencies to achieve the best quality of calibrated data in air pollution sensors. However, in most of these works the nodes were continuously energized, without running on batteries, and saving energy consumption was not an objective. Note that in air pollution sensors, a sampling rate of a few seconds is considered a high sampling rate, while sampling rates in the order of minutes are considered low sampling rates.

³The terms power consumption and energy consumption are used interchangeably throughout the paper.

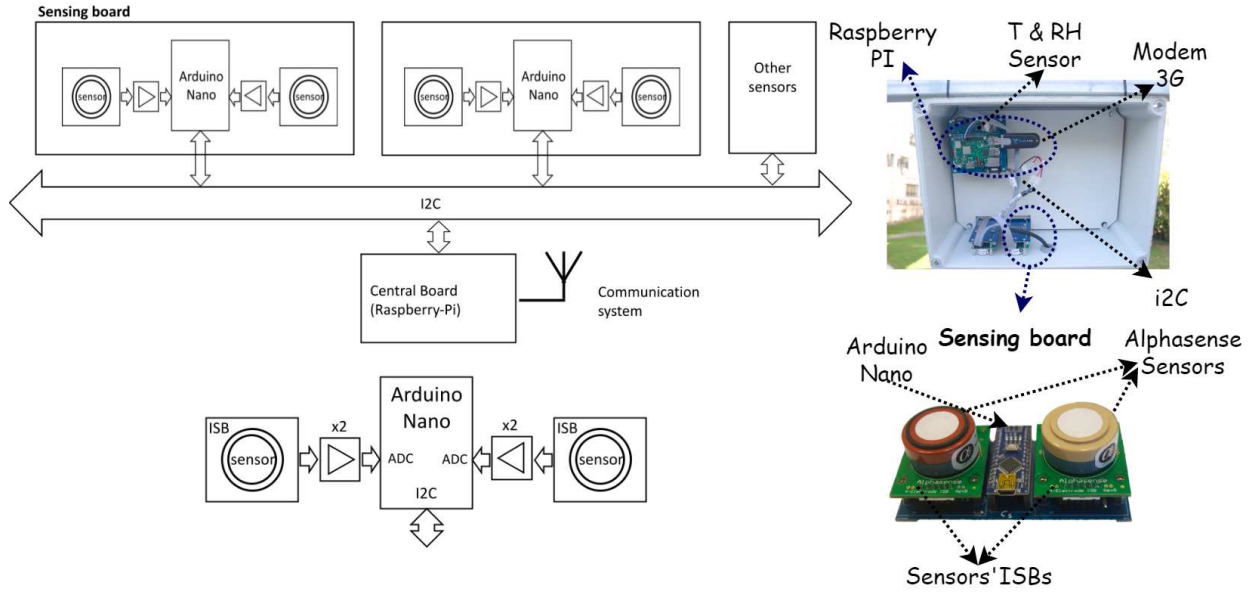


Fig. 1. Air pollution data capture prototype Captor node on top, and the Captor's sensing board on bottom.

Our work: In this paper, we study the impact of the sampling frequency of air quality sensors on the calibration quality and duty cycle. In this way, we provide valuable information for professionals who want to build a node to measure air pollution and require energy savings in the sensor subsystem. This paper is not about the the study of energy saving methods for the communication subsystem, which has been extensively investigated in the literature.

III. SENSING NODE: THE CAPTOR NODE

To carry out the study we have developed a data capture node, Captor, whose purpose is to attain maximum flexibility and scalability to integrate sensors, and to be able to experiment with different duty cycle strategies and sampling frequencies.

A. CAPTOR node

The Captor node is built based on an I2C bus, to which different sensing subsystems, and a master central node, which is in charge of managing a communication subsystem, are attached; see Figure 1. In the specific case of the data reported in this work, a gas monitoring shield designed to integrate two Alphasense sensors is used, see Figure 1. The sensing board is built using an Arduino Nano microcontroller unit (MCU), which samples the data measured from two gas sensors, and a temperature and relative humidity sensor. Each gas sensor is supplied by the manufacturer with an individual sensor board (ISB) [28]. The output of the ISB is further amplified by a factor of x2, in order to reduce quantifying errors, and sampled by the analog-to-digital converter (ADC) of the Arduino Nano MCU. The sensor sampling frequency is set to 0.5 Hz. The data captured by the Arduino Nano MCU is periodically sent through the I2C bus to the central processing unit, based on a Raspberry Pi node, which also handles the communications subsystem. The node is designed to scale the number of

sensors included by adding new sensing boards connected to the I2C bus.

B. Low-cost sensors

To carry out this work, Alphasense electrochemical gas sensors were used. Specifically, we use OX-B431 O₃ sensors [29], NO2-B43F NO₂ sensors [30], and NO-B4 NO sensors [31]. The B4 sensor family, designed for use in urban air fixed site networks, is a 4-electrode (working, reference, counter and auxiliary) electrochemical sensor with very low parts per billion (ppb) detection levels. Each sensor is provided with an individual sensor board (ISB) [28] that requires 3.5 to 6.4 stable DC supply with a consumption around one milliamp. To measure a pollutant, the ISB sends two raw values to a 10-bit ADC: the working electrode (WE) is the reduction or oxidation site of the chosen gas species, and the auxiliary electrode (AE) is used to correct for zero current changes [17]. The final raw signal is obtained by subtracting the raw working and auxiliary values produced by the ADC, S=WE-AE, or by feeding both parameter values, WE and AE, to the machine learning algorithm as separate features. The O₃ sensor is a special case, since the working electrode measures O₃ and NO₂ simultaneously. This means that to obtain O₃ it is necessary to use a pair of OX-B431 O₃ and NO2-B43F NO₂ sensors. Furthermore, it should be noted that the manufacturer of these sensors indicates that they have a response time T_r of less than 80 seconds for O₃ and NO₂ [29] [30] and 45 seconds for NO [31]. This is important for the implementation of strategies that minimize the duty cycle of the sensing subsystem, since it is necessary, for example, to wait at least 80 seconds for O₃ and NO₂ before obtaining valid measurements from the sensors.

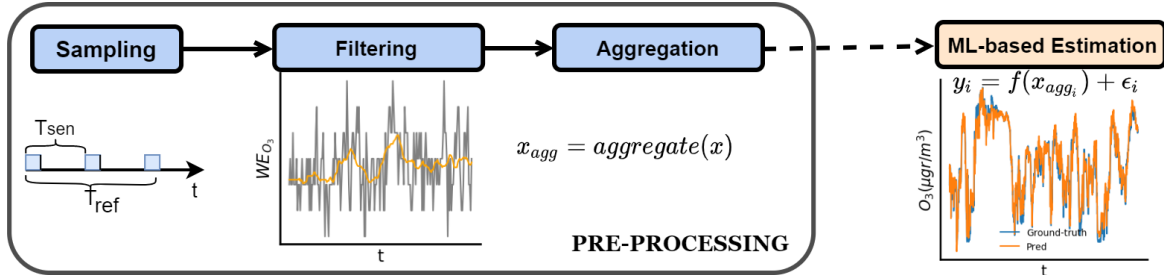


Fig. 2. Sensor data gathering pipeline: from sensor sampling to machine learning estimation.

C. Data sets

This section describes the data sets obtained from Captor node prototypes that are later used for the experiments in section V. Two Captor nodes were deployed during four months at a reference station in Barcelona (Spain). Captor node labeled as 20001 mounted one Alphasense OX-B431 O₃ sensor, one Alphasense NO2-B43F NO₂ sensor, one Alphasense NO-B4 NO sensor, and a DHT-22 temperature and relative humidity sensor. Captor node labeled as 20002 mounted one Alphasense OX-B431 O₃ sensor, one Alphasense NO2-B43F NO₂ sensor, and a DHT-22 temperature and relative humidity sensor. This way, these data sets allow the study of sampling strategies and sensor calibration for three different air pollutants. Given the availability of high-frequency measurements (0.5Hz), different sensor sampling policies can be simulated by subsampling these data sets⁴.

TABLE II
DATA SETS USED FOR THE EXPERIMENTS.

Node Label	Sensor	Deployment Period	T _s
20001	O ₃	2021/01/15 - 2021/05/15	2s
	NO ₂	2021/01/15 - 2021/05/15	2s
	NO	2021/01/15 - 2021/05/15	2s
20002	O ₃	2021/01/15 - 2021/05/15	2s
	NO ₂	2021/01/15 - 2021/05/15	2s

Each of the low-cost electrochemical sensors provides measurements from the working electrode (WE) and auxiliary electrode (AE) in ADC units. The temperature sensor collects measurements in degrees Celsius (°C), and the relative humidity sensor collects measurements in percent humidity (%). Table II summarizes the different sensor data used in the experiments. These two nodes were deployed from 2021/01/15 to 2021/05/15. Reference station's values are available hourly, so the reference data period T_{ref} is equal to one hour. The time required to sample a sensor measure using these sensing nodes is 2 seconds (T_s=2s). The reference station data can be downloaded at the government's open data web⁵, while the raw sensory data are available at [32] with a further data description.

⁴We emphasize that the sensing boards were not put to sleep, and therefore, the effect that turning the sensor on and off may have on aging or sample quality has not been studied.

⁵ Reference station data provided by the website of the regional government

IV. SENSOR DATA GATHERING PIPELINE

In this section, we show the different steps required to obtain air pollution estimates from low-cost sensors. The whole sensor data gathering process can be divided into two stages; sensor data pre-processing, and the estimation of pollutant concentrations using a supervised machine learning algorithm. All data pre-processing can be performed at the sensing node, so that only measurements synchronized with the reference values are transmitted to the cloud, and the subsequent estimation of pollutant data is performed off-line. It is important to note that to estimate the final pollutant concentration, the machine learning algorithm, as described in section IV-B, uses a combination of samples taken by several sensors of the same node. That is, for example, to estimate the value of O₃ we need to combine the sensor measurements of O₃, NO₂, temperature and relative humidity. This edge computing approach significantly reduces the amount of data transmission required, since only the aggregation of collected data is sent to the cloud. From now on, we focus on how to reduce power consumption in the sensing subsystem when taking samples. Figure 2 illustrates all the required pre-processing steps to be able to perform the sensor data gathering procedure.

Since we want to mimic the sampling process of the reference station, we could be tempted, if the station provides hourly data, to sample twice as much by Nyquist's theorem, that is to measure every thirty minutes. Nevertheless, the problem is different, since the value provided by the reference station every hour is the aggregation of different values collected during this interval, it is not a single sensor sampling measure. Therefore, the goal is to use a data gathering process similar to that of the reference station, with its respective sampling and aggregation stages, to produce data as similar as possible to those of the reference station.

A. Pre-processing

Data pre-processing has a big impact on the subsequent representation of the data. As mentioned above, having the data synchronized with reference stations, in the environment where the node will be deployed, allows to calibrate the sensors, and to detect drifts, aging or outliers [33], [34], which will lead to a recalibration of the sensor. Specifically, we divide the pre-processing operation in three stages; the sampling of the sensor, the filtering of the collected samples, and the aggregation of these samples.

The process of taking measurements in air pollution sensors is as follows, Figure 2: the node takes a value of the sensor every T_{sen} seconds. For this value to be representative, it may be necessary to wait a sensor response time T_r , take a sequence of N_s measurements, apply a filtering algorithm to remove outliers and smooth the measurements, and finally aggregate them into the sample T_{sen} . The microcontroller can go into sleep mode until it has to collect samples again, and switch off the sensing board if necessary. The node manages an array of sensors, each with its electronic board, whereby the node reports each T_{sen} a vector containing air pollution sensor values (e.g., NO_2 , O_3 , NO) and environmental values (e.g., temperature and relative humidity). Two strategies are possible: i) a packet is generated with the sample vector every T_{sen} , or ii) if energy savings are desired in the communication subsystem, and the application only needs values every T_{ref} , a second aggregation is performed and the measurement vector is transmitted every T_{ref} . The data capture process is detailed below:

1) ***Sensor sampling***: At this stage, the N_s samples that are part of the representative sample T_{sen} are taken. We focus on taking samples from a single sensor. In the case of having an array of sensors the microcontroller can run the sampling process in parallel, activating all the sensor boards simultaneously and polling them with a round robin strategy. Besides, since different sensors are attached to different sensing boards, a specific sampling strategy per sensor can be designed.

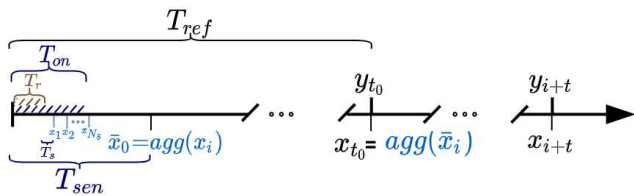


Fig. 3. Sensor sampling scheme.

To obtain the value at instant T_{sen} the microcontroller wakes up the sensor board and takes N_s consecutive samples. In this case, the duty cycle is $N_s T_s$ over T_{sen} . However, there are air pollution sensors, for example, the ones used in this article that have a response time of T_r , so it is necessary to wait T_r before collecting valid measurements. Indeed, this response time may vary from one sensing technology to another, in fact, it can be seen as a user-defined parameter to specify the amount of time to wait before collecting a measure in order to prevent the collection of incorrect measurements. Summarizing, the microcontroller wakes up the sensor board, waits for a time T_r and then takes N_s consecutive samples to build the value T_{sen} and turns off the sensor board. In this general case, the duty cycle DC is given by:

$$\begin{aligned} \text{DC} &= \frac{T_{on}}{T_{sen}} \\ T_{on} &= T_r + (N_s \cdot T_s) \\ T_{on} &< T_{sen} \end{aligned} \quad (1)$$

TABLE III
SENSOR SAMPLING PARAMETERS.

Parameter	Definition
T_s	Required time to take a sensor measure
T_{sen}	Sensing node sampling period
N_s	Number of samples taken every sampling period
T_r	Sensor response time before valid measurements
T_{ref}	Reference data period
DC	Sampling strategy duty cycle
T_{on}	Time the MCU is switched on to measure

The number of samples N_s that make up the value generated by T_{sen} impacts the duty cycle of the sensing subsystem and the quality of the data estimated by the machine learning algorithm. The adjustment of the value of T_{sen} has an impact on the number of packets to transmit, on the duty cycle of the sensor subsystem, and on the quality of the value estimated by the machine learning algorithm. Table III summarizes the different sampling parameters used throughout the paper.

2) **Filtering:** Once N_s sensor samples have been collected each sensing node's sampling period T_{sen} , these must be filtered in order to remove outliers and smooth the data. One of the most common techniques for removing outliers in sensory data is the use of the z-score [18]. Assuming that the collected measures follow a Gaussian distribution the z-score is computed as:

$$z(x) = \frac{|x - \bar{x}|}{s_x} \quad (2)$$

Where \bar{x} and s_x are the sample mean and sample standard deviation. Then, the z-score is thresholded in such a way that values greater than 2 are removed. Other signal filtering techniques (e.g., moving average) can be useful to eliminate abrupt changes in the signal and smooth the data tendency. For instance, Mijling *et al.* [13] eliminates samples that deviate a given percentage from the sample mean. The filtering process is necessary because the signals measured by the sensors are noisy and tend to produce outliers, in which case the subsequent aggregation would be affected and, consequently, the quality of the estimated data would be degraded.

3) **Aggregation:** In the aggregation stage, the sensor data, after filtering, are aggregated into a single measurement period T_{sen} . The most common statistics used for the aggregation are the sample mean and median. However, these statistics require a certain number of samples in order to not be biased, so after the filtering step it is important to check whether the resulting number of samples in a period is large enough for averaging, if not, the resulting mean may not be representative and the sample is discarded producing a gap.

The measured value is now included in a vector of measurements from all sensors on the node, and can be transmitted to the cloud where the machine learning algorithm can estimate the pollution value with granularity T_{sen} . The reference stations, being connected to power supply, usually take continuous T_{sen} values and aggregate those values to hourly values ($T_{ref}=1h$), which are the ones displayed in the applications. If we want to save energy in the communications subsystem, we can do a second aggregation with the T_{sen} values to match

the values of the reference stations T_{ref} values. This allows to have a heterogeneous network of reference stations and low-cost sensor nodes that can spatially measure a pollutant in an area as the two types of nodes have the same time granularity.

However, nodes with low-cost sensors that have a response time of more than a minute, and that also use batteries and implement a duty cycle to save energy in the sensing subsystem, will not be able to produce T_{sen} values in the same way as reference stations. In this work, we investigate different ways to implement such a duty cycle, from a strategy that tries to mimic as much as possible, given the constraints of the low-cost sensors, a reference station, to a more aggressive strategy that although it does not follow the same dynamics as a reference station, produces an aggregated value at the T_{ref} instant saving the maximum energy. The objective is to study the compromise between the quality of the data generated by the estimation process of the machine learning algorithm, and the achievement of a duty cycle that saves the maximum energy in the sensing subsystem and in the transmission subsystem, considering energy savings in the latter subsystem, such as minimizing the number of packets to be transmitted.

The most aggressive strategy that can save more energy is to consider that the value taken in T_{ref} only considers a T_s value. However this value may be unrepresentative of the physical phenomenon during the whole T_{ref} interval. The less aggressive strategy, which saves less energy and better mimics the reference station is to consider that during T_{ref} , we have as uniformly as possible $N_s[T_{ref}/T_{sen}]$ measurements. In the results section, we will review the two strategies, where the N_s samples are taken uniformly in T_{sen} or are taken consecutively in T_{sen} assuming a sensor response interval T_r , and thus, showing their feasibility and implications in terms of data quality and power consumption.

B. Machine learning-based sensor calibration

To estimate the values of an air pollutant we use calibration techniques based on machine learning. To this end, we need the sensing node to produce values with the same granularity T_{ref} as the reference station in order to compute the coefficients or hyperparameters of the machine learning algorithm. The process of obtaining these coefficients or hyperparameters is called sensor calibration [3], [4]. Once the sensor is calibrated, the future estimated values can have a T_{sen} or T_{ref} granularity depending on the intended application of the sensor network. Several machine learning techniques [5], [9], [35], [36] have been used to improve the accuracy of the calibration and to obtain air pollution measurements from the raw values of the sensors. Ultimately, sensor calibration is reduced to a supervised problem where we have the pairs $\{\mathbf{x}_i, y_i\}_{1,..,N}$ where $\mathbf{x}_i \in \mathbb{R}^P$ are the sensor values, where P is the number of sensors included in the calibration, and $y_i \in \mathbb{R}$ are the corresponding reference values. As an example, for calibrating an electrochemical Alphasense OX-B341 O_3 sensor, we need the raw values from an Alphasense OX-B341 sensor, an Alphasense NO2-B43F NO_2 sensor, a temperature sensor and a relative humidity sensor [5], [13], [15], [17], [37].

That means that the vector \mathbf{x} has dimension four. Given these data, we can formulate the following problem:

$$y_i = f(\mathbf{x}_i) + \epsilon_i; \quad \forall i = 1,..,N \quad (3)$$

Where $f(\cdot)$ is the function to be determined by machine learning, and ϵ is the error assumed to be independent and identically distributed. There are different algorithms to estimate the function $f(\cdot)$, among which we have the multiple linear regression. The MLR assumes that the response variable varies linearly depending on the sensor values so (3) can be rewritten as:

$$y_i = \boldsymbol{\beta}^T \mathbf{x}_i + \epsilon_i; \quad \forall i = 1,..,N \quad (4)$$

Where $\boldsymbol{\beta}$ is the vector of coefficients to be found by solving the problem by least squares. Other more complex techniques based on nonlinear modeling have been used including K-nearest neighbors, random forests, support vector regression or artificial neural networks [5], [9], [24], [37].

V. RESULTS

In this section, we perform three different experiments to evaluate the impact of the sampling strategy on the *in-situ* calibration of low-cost sensors using the data sets described in section III-C:

- (A) we analyze which are the most important sensors to include in the sensor calibration, by means of a feature selection, investigating their impact on the calibration accuracy. To achieve this, we perform a forward stepwise feature selection using 10-fold cross-validation (CV), thus adding the variable that increases the R^2 the most at a time.
- (B) we perform sensor calibration, for the O_3 , NO_2 and NO sensors, using the best subsets of sensors found with the highest data availability ($T_{sen}=2s$), therefore assuming no energy consumption restrictions.
- (C) we investigate the impact of the sensor sampling parameters on the sensor calibration accuracy and power consumption. To this end, we compare different sampling periods for the sensing node T_{sen} , as well as different number of samples collected in these periods N_s . We also consider sensor response periods. A 10-fold CV is performed for every sampling setting, discussing the resulting goodness-of-fit metrics, duty cycles and power consumption implications.

To evaluate each one of the experiments 75% of the data set is used as training set, and the remaining 25% is used as test set. Moreover, the different data set are shuffled so that the different experiments can be evaluated without the effects of the changing environmental conditions.

A. Feature selection for O_3 , NO_2 and NO sensor calibration

Performing feature selection is key to select which sensors have to participate in the process of sensor calibration and pollutant estimation. On the one hand, the sensor manufacturer Alphasense mentions that to measure O_3 with the OX-B431 sensor it is necessary to include the NO_2 measurements of

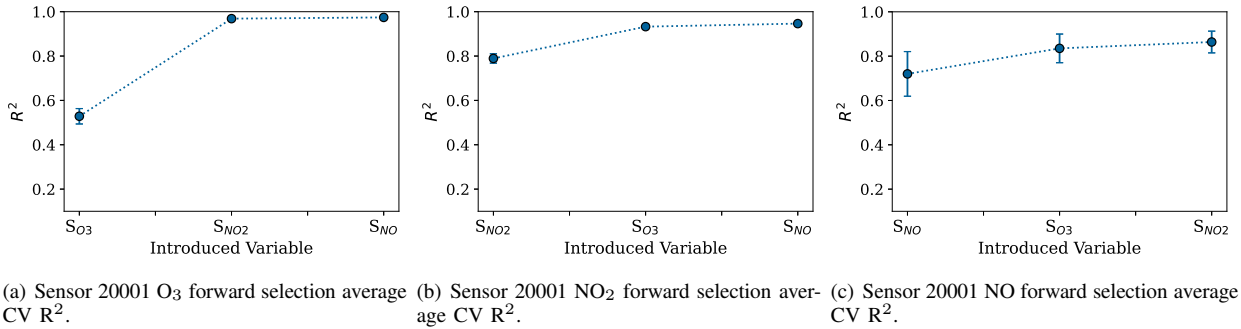


Fig. 5. Forward feature selection for the different sensors. Horizontal axis indicates the variables added to the model from left to right. Bands indicate average CV R² 95% confidence interval.

the NO₂-B43F sensor, since the OX-B431 sensor measures the sum of O₃ and NO₂. On the other hand, it is interesting to observe whether the NO₂ or NO calibration benefits from the O₃ sensor, since it is known that the tropospheric ozone phenomenon has a cross-correlation with the types of nitrogen oxides. Thus, there are two factors that condition the improvement of sensor calibration as a function of the sensors introduced in the calibration; the underlying sensor technology used, and the cross-correlations and sensitivities present. Finally, it is known that the O₃, NO₂ and NO sensors are very sensitive to changes in temperature and relative humidity, acting as correctors of the measurements in the predictive model [3]–[9], [13], [15], [17], [24], [25], [37].

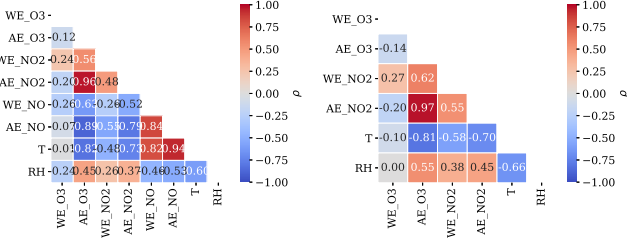


Fig. 4. Correlation maps for nodes 20001 and 20002.

To better observe the behavior of the different sensors, Figures 4.a) and b) show the correlations between the sensors of the two Captor nodes. As explained in section III-B, to read electrochemical sensors correctly, the working electrode (WE) and the auxiliary electrode (AE) need to be subtracted, $s_i = WE_i - AE_i$, for sample i -th. Correlation maps, Figures 4.a) and b), show how the different auxiliary electrodes correlate with each other, since they indicate the base conditions on which the sensor has to be corrected. For instance, in Captor 20001, Figure 4.a), it can be observed how the internal temperature is related to the auxiliary electrodes, as its correlation with them is strong.

It is also interesting to see what other contaminants may benefit the calibration of a particular sensor. Many contaminants can benefit from other contaminants given the cross-correlations and cross-sensitivities present. For example, the Alphasense O₃-B4F measures O₃ and NO₂ together, so the

manufacturer specifies that to obtain correct ozone measurements both sensors must be subtracted. Here we show an experiment, where using multiple linear regression, we add sensors in the calibration to see what the different pollutant sensors can contribute, assuming that the meteorological sensors (S_T and S_{RH}) are always included. So, in order to obtain the best features for each sensor model we perform a greedy forward feature selection, which is a wrapper method where we start with the sensor that has the best performance in terms of coefficient-of-determination R², then we add the next sensor that increases the most the performance and so on. This is performed using a 10-fold cross-validation procedure to obtain a generalist R² measure. As it can be seen in Figure 5.a), the O₃ calibration using only the O₃ sensor does not perform well (R²=0.53), as mentioned, the NO₂ measures need to be introduced to eliminate its effect over the O₃ sensor, so adding the NO₂ sensor increases the cross-validation R² from 0.53 to 0.97. No other sensor can be added to the model to further improve its performance. So, the best models corresponds the O₃ calibration using the O₃ sensor, the NO₂ sensor, the temperature and relative humidity sensors. The NO₂ calibration results are slightly different, Figure 5.b), the R² obtained is 0.79 using only the NO₂ sensor. Then, adding the O₃ sensor improves the model (0.93 R²), given that these are anti-correlated phenomena. Lastly, the NO sensor seems to improve very little the model's performance. Therefore, the NO₂ sensor can be calibrated using the NO₂ sensor, the O₃ sensor, the temperature and relative humidity sensors. For the calibration of the Captor 20001 NO sensor, Figure 5.c), the NO sensor alone is capable of achieving a R² of 0.72, and given the variability of the NO calibration, the confidence intervals are the largest of the three cases. The tropospheric ozone sensor increases the performance from 0.72 to 0.84 CV R², while the NO₂ sensor slightly increases the coefficient of determination. In short, the NO sensor calibration requires the NO sensor, the O₃ sensor, the temperature and relative humidity sensors.

B. Machine learning-based calibration

Given the aggregated sensor data, synchronized with the reference data, sensor calibration can be performed using machine learning techniques. This is the ultimate step in obtaining air pollution estimates using low-cost sensors. All pre-processing steps have the sole objective of obtaining good

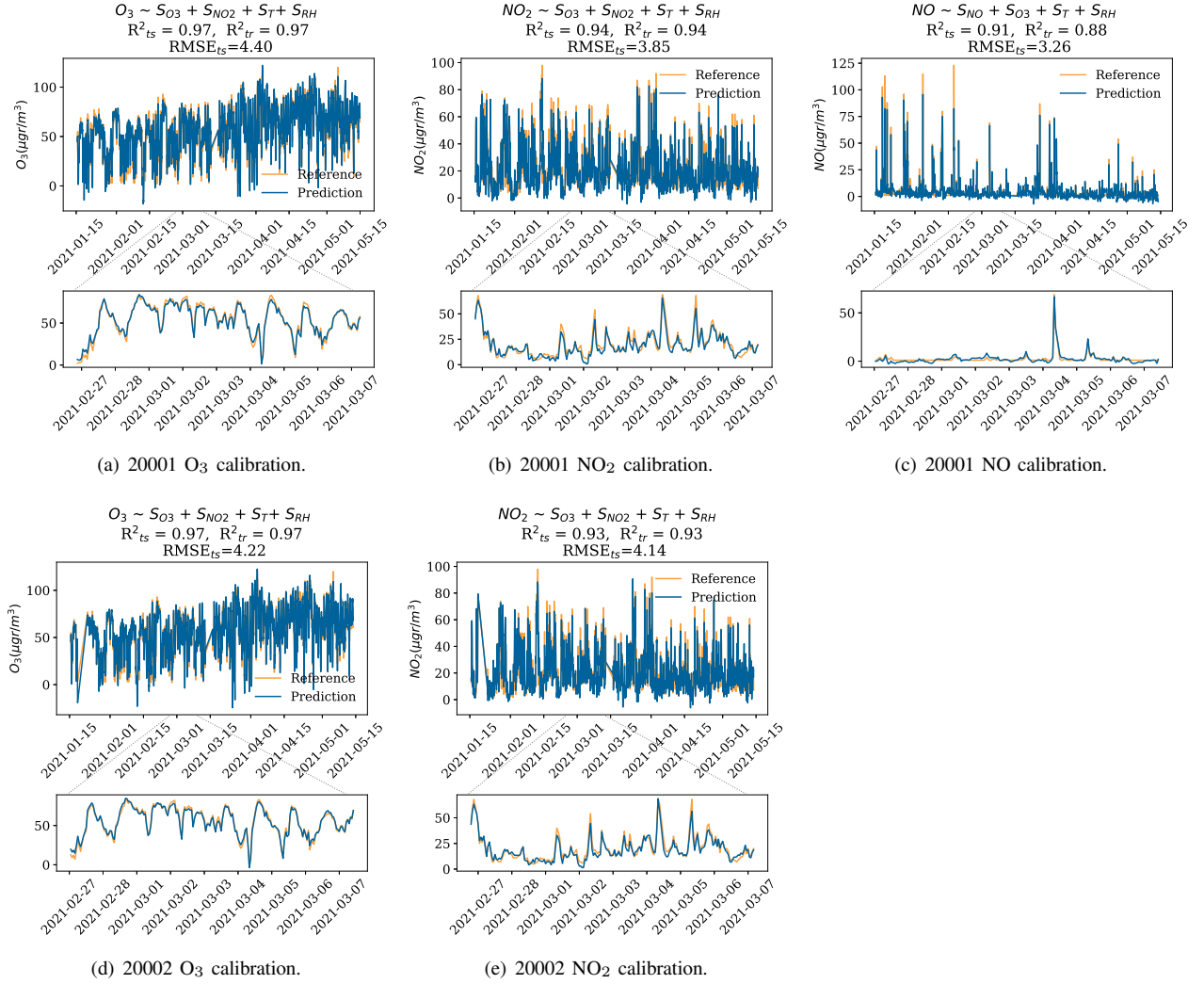


Fig. 6. Calibration results for the O₃, NO₂ and NO sensor of Captor nodes 20001 and 20002.

quality raw measurements for the purpose of performing a good calibration of the sensors, and therefore producing high-quality estimations of air pollution concentrations. In this section, we show the results of calibrating the different sensors using the best subset of sensors obtained in section V-A with the highest data availability. Therefore, we show the best case of having the sensing node connected to a power supply, so collecting sensor measurements uniformly every two seconds. In this way, we can show the ability of the different sensors to predict the real air pollutant concentrations in the case of not having energy restrictions.

Figures 6.a) and d) show the results of the calibration of the two O₃ sensors using the multiple linear regression model. As it can be seen, the test R²'s are very good, specifically 0.97 in both cases, with root-mean-square errors (RMSEs) of 4.40 and 4.22 µgr/m³. Hence, the resulting models using the subset of sensors for O³ calibration have a very good performance. Similarly, Figures 6.b) and e) show the calibration results for the two NO² sensors, where the models obtain a testing R² of 0.94 and 0.93, with RMSEs of 3.85 and 4.14 µgr/m³. This case is interesting since the nitrogen dioxide concentrations are quite high, with peaks up to 100 µgr/m³. And finally, Figure

6.c) shows the calibration for the Captor 20001 NO sensor, with a testing R² of 0.91 and a testing RMSE of 3.26 µgr/m³. The NO calibration depends a lot on the data used for calibration and testing, since NO has very abrupt peaks, it is that the NO concentrations are most of the time low but sometimes it has very high peaks. Hence, the calibration goodness-of-fit depends on the pollution peaks observed during the calibration period and testing period. This has already been observed in the results of the previous section, where the average CV R² for NO had the largest confidence intervals of the three cases.

In some cases, the calibration by multiple linear regression may not work as well as in this case. Then, nonlinear calibration techniques (see related work II) can be used to better fit the calibration models, and to obtain better air pollution estimations. Next section studies how the quality of this calibration varies using different data acquisition strategies.

C. Sensor sampling impact

As cited in the literature (section II), deployed nodes used a wide variety of sampling rates (from 1 second to 10 minutes) without considering the implications on power consumption.

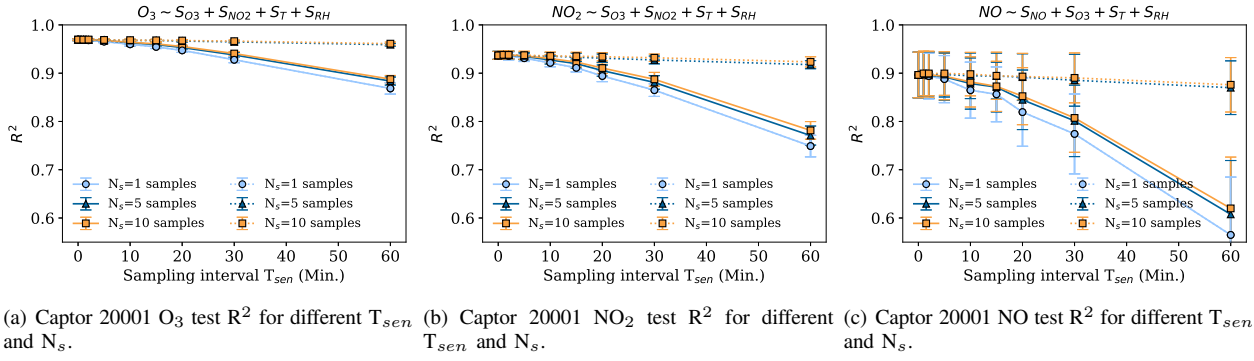


Fig. 7. Average CV R^2 and 95% confidence intervals for different sampling settings; sampling period T_{sen} and number of consecutive samples N_s taken every period T_{sen} . The solid lines denote the strategy that the N_s samples are taken consecutively after a sensor response period, and the dotted lines denote the strategy that the N_s samples are taken uniformly at T_{sen} .

None of the work found has explained the impact of varying the sampling period used on sensor calibration or on node power consumption. Therefore, in this experiment we explore the impact of the sampling period T_{sen} and the number of samples collected N_s on the model's accuracy, and the implications of the resulting duty cycles with respect to the power consumption of the sensing node. The different sampling strategies are simulated by subsampling the data sets measurements. Since reference values are available hourly, the periods T_{sen} tested are less than or equal to one hour $T_{sen} \leq 1h$.

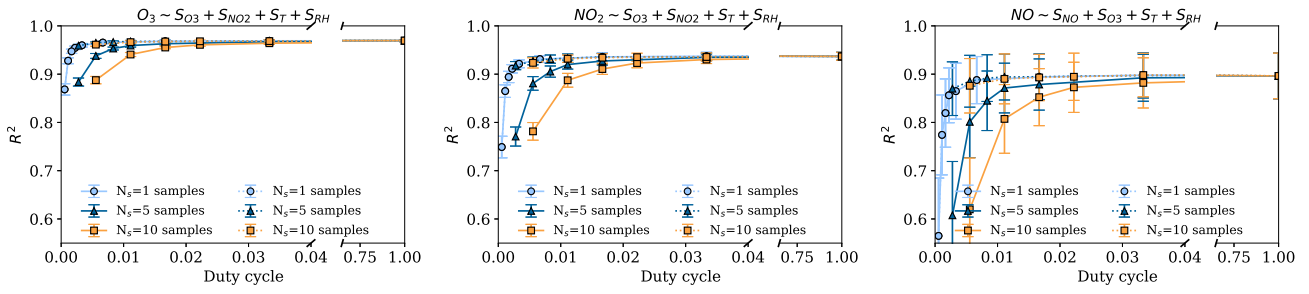
1) **Impact of node sampling period T_{sen} :** The following experiment shows the result of calibrating the sensors by subsampling the measurements with different sampling periods T_{sen} , from 2 seconds and 1 minute, to 60 minutes. Obviously, the fact of sampling the sensor fewer times makes the measurements less reliable, as the data aggregation will consist of fewer samples. Besides, we compare two strategies, one consisting of taking the N_s samples uniformly over T_{sen} , only possible when the sensor's response time is small or negligible, and the other consisting of taking N_s consecutive samples in T_{sen} after a sensor response period.

Figure 7.a) shows the average CV R^2 and the confidence intervals for applying different periods T_{sen} and N_s samples to the O_3 calibration. As it can be seen, in the case of sampling consecutively (solid lines), there is very little worsen in performance from sampling every minute to sampling every 10 minutes. From this point, the R^2 starts to decrease until it reaches an average CV R^2 of 0.87. In the case of the 30-minute and 60-minute periods, it should be noted that the sensor is only being sampled twice or once (for $N_s=1$) per T_{ref} , so the accuracy may decrease considerably. The difference between taking one, five or ten samples is not significant until we sample every 30 to 60 minutes. However, as expected, when we take few samples, e.g., $N_s=1$, the confidence intervals are worse, meaning that the quality of the calibration can exhibit variability when only sampling once. We note as an example, that in case of having $T_{sen}=5min$, the aggregation when calibrating at $T_{ref}=60min$ is of 12 values. This indicates that, in the case of frequent sampling (e.g., $T_{sen} \leq 5min$), it is not necessary to take more than one sample, but when only sampling fewer times T_{sen} per reference period T_{ref} , even if

more than one sample is taken, the quality of the calibration is not maintained, since the subsequent aggregation, even if it has more samples in total, these are taken too consecutively in unrepresentative instants. For instance, if $T_{ref}=30min$ and $N_s=10$, there are 20 samples participating in the aggregation at instant T_{ref} (more than the 12 samples with $T_{sen}=5min$ and $N_s=1$) but they are less representative. In other words, it is better to sample with fewer samples but more distributed over the period T_{ref} , than to sample with more samples consecutively but fewer times at T_{ref} .

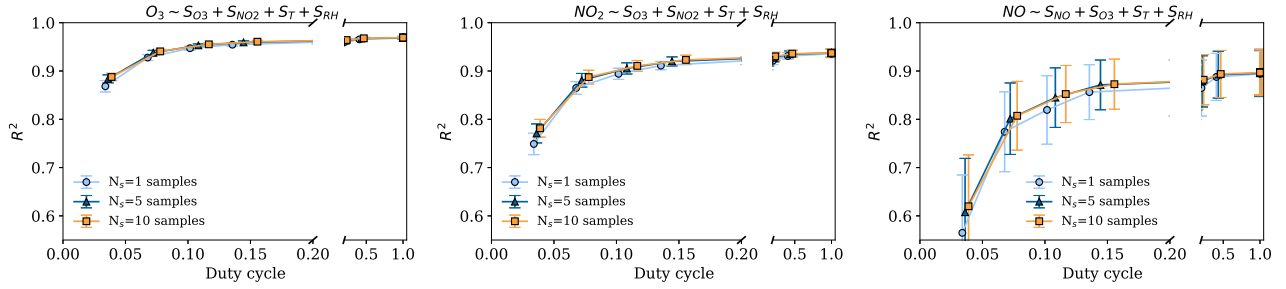
Figure 7.b), case of consecutive sampling, shows a similar pattern for the NO_2 sensor, but with a larger decrease in R^2 for large sampling intervals. Indeed, the R^2 is observed to remain almost constant for $T_{sen} \leq 10min$, with values around 0.94. However, the worsening in this case is much greater than in the case of O_3 , since at $T_{sen}=30min$ the R^2 is reduced to 0.86, and at $T_{sen}=60min$ to 0.75. Regarding to the number of samples taken every period, it is seen that one sample is not significantly enough, so this sampling setting works worse than the others for sampling intervals larger than 10 minutes. In addition, since NO_2 is a less smooth signal than O_3 , with few samples per T_{sen} interval, there is greater variability, which explains the higher confidence interval values for $N_s=1$. Finally, for the uniform sampling approach is the same for NO_2 as for O_3 , where five to ten uniform samples over T_{sen} obtain very good data quality.

Figure 7.c) shows the results for the NO sensor calibration. In this case, NO is a phenomenon that naturally presents more abrupt changes in the measurements, already seen in the confidence intervals of the feature selection experiment (section V-A), which causes the different calibrations to have large confidence intervals. The same decreasing trend is observed as in the cases of O_3 and NO_2 R^2 , where from $T_{sen}=10min$ the R^2 starts to decrease, and it is also observed how the R^2 depends strongly on the number of samples taken since the gap in performance between taking one sample and five is the largest of all three pollutants. The NO signal contains many peaks, so that even sampling N_s samples in a row for an instant that does not pick up such peaks may be unrepresentative. Another effect is the uncertainty we will have in the measurements. In those cases where the number



(a) Captor 20001 O₃ test R² for different duty cycles. (b) Captor 20001 NO₂ test R² for different duty cycles. (c) Captor 20001 NO test R² for different duty cycles.

Fig. 8. Average CV R² and 95% confidence intervals for different duty cycles with negligible sensor response time (T_r=0). Solid lines denote the strategy that samples the N_s consecutively, and the dotted lines denote the strategy that samples the N_s uniformly at T_{sen}.



(a) Captor 20001 O₃ test R² for different duty cycles. (b) Captor 20001 NO₂ test R² for different duty cycles. (c) Captor 20001 NO test R² for different duty cycles.

Fig. 9. Average CV R² and 95% confidence intervals for different duty cycles with a sensor response time equal to 2 minutes (T_r=2min.).

of samples is small, e.g., N_s=1, the confidence interval is very poor, precisely because of the high variability of the data. This interval improves when taking more samples, even if the measurement point is not very representative, and the R² decreases, the confidence interval decreases. Therefore, in the case of signals with high variability, high bandwidth, it is logical to sample at more points. In the case of sampling uniformly, the same trend as for the two previous pollutants is observed, where taking at least five uniform samples are enough to maintain the highest data quality. From all this, we can conclude that it is better to take more than one sample N_s>1 if the sampling period is large (T_{sen}≥10min), so that the aggregation is more representative. But, in the case of having a lower sampling period fewer samples are enough to obtain a high R² since the aggregation at each T_{ref} will contain enough samples to be representative.

An important conclusion from these results is that different sensors may need different sampling strategies to maintain similar data quality in the prediction phase if energy savings are to be achieved. For instance, the performance gap between sampling five uniform samples for T_{ref}=30min and five consecutive samples for T_{ref}=30min is of 0.02 R² in the O₃ case, 0.05 R² in the case of the NO₂, and 0.08 R² in the NO case.

2) **Impact of duty cycle DC: Data Quality:** Now, we compare the data quality implications of the different sampling policies with respect to the duty cycles, which will have different energy consumption consequences. We explore two

possible cases; negligible sensor response time T_r=0 and response time equal to two minutes T_r=2min, given that data sensor responses may take up to 80 seconds, see section III-B. We assume that the time to turn on and off the sensing device is negligible. Figures 8.a), b) and c) show the R² with respect to the duty cycle with no response time. Figure 8.a) shows the results for the O₃ sensor, where it can be seen that since there is no sensor response time there is no penalty for turning on the node too many times. Indeed, for similar duty cycles, the strategy that takes one single sample frequently is able to achieve a R² of 0.96, while the strategy that samples five measurements in a row achieves a R² of 0.89 with a similar duty cycle. Sampling strategies that sample more than one measure have larger duty cycles since the sensing node needs to remain measuring more time. Regarding the uniform sampling strategy (dotted lines), it is observed that with N_s=5 samples is able to achieve a very good goodness-of-fit at a very low duty cycle. However, this case is not representative at all, since the sensor's response time will almost never be negligible and the presence of a sensor response time makes the strategy of sampling uniformly infeasible. Figure 8.b) shows the same results for the NO₂ sensor, again the same results are seen, where for similar duty cycles the strategy that takes one single measure obtains a R² of 0.93 while the strategy that takes five samples obtains a R² of 0.75. That is, the setting {T_{sen}=15min, N_s=1} works much better than the setting {T_{sen}=60min, N_s=5} with similar duty cycle. Figure

8.c), shows the results for the NO sensor, with exactly the same pattern but with worse average performance and larger variability because of the variability of this fast-changing phenomenon.

The results of the duty cycle for a 2-minute sensor response time ($T_{ref}=2\text{min}$) and therefore with a $T_{sen} \geq 2\text{min}$ are shown below. Here, only the results of the strategy that takes the measurements sequentially are shown, since with a sensor response time of two minutes it is no longer possible to take samples uniformly as the node would always be powered on. Recall that low duty cycles correspond to large T_{sen} and fewer samples taken in the interval T_{ref} . This can be seen in Figures 9.a), b) and c), where lower R^2 are obtained for low duty cycles. The duty cycles start to stabilize at DC=20% ($T_{sen}=10\text{min}$). When the physical phenomenon presents great variability, as in the case of NO, the confidence intervals are poor. However, large T_{sen} periods with one single sample introduce more variability, as observed in the confidence intervals of sampling strategies with $N_s=1$. In this case it is better to take more samples, which slightly increases the duty cycle, since the sensor response time is the one that dominates the duty cycle.

3) Impact of duty cycle DC: Power Consumption: The case of a negligible sensor response time may not be the most usual case in a low-cost air pollution node. In particular, the sensor response time of the node may vary between different processing and sensing technologies. The implications of a higher or lower duty cycle on the power consumption of a node depend on the different components used by the node. However, we can assume that the power consumption of the node is directly given by the duty cycle, as it is the ratio between the time it is powered on during the sampling period (T_{on}) and the sampling period (T_{sen}). Furthermore, depending on the consumption of the different components, one can decide to send to sleep mode only the microcontroller, or sending microcontroller to sleep and switching off the sensors.

Now, looking at the results for the duty cycle with sensor response time, Figures 9.a), b) and c), it can be observed that with a duty cycle of about 0.10 the quality of the calibrations in all three cases (O_3 , NO_2 and NO) are stable, introducing very little improvement at higher duty cycles rates. This means that a calibration almost as good as when the node is always on (DC=1) can be obtained with a duty cycle about ten times smaller (DC=0.10), therefore reducing the power consumption very significantly. This is of vital importance for cases where nodes powered by batteries are used, where the sensing node cannot always be connected and there are power consumption restrictions. Table IV shows the average CV R^2 for all the tested sensors and different duty cycles obtained (with sensor response time equal to two minutes) using different sampling strategies; duty cycles equal to 1.0 ($\{T_{sen}=2\text{s}, N_s=1\}$), 0.10 ($\{T_{sen}=20\text{min}, N_s=1\}$), and 0.03 ($\{T_{sen}=60\text{min}, N_s=1\}$). As it is observed, for duty cycles of 0.10 the sensor calibrations worsen by about 0.02-0.08 R^2 , in the worst case, the NO sensor drops from 0.90 to 0.82 R^2 . On the other hand, in the extreme case where the node is only powered on once, with a resulting duty cycle of 0.03, the R^2 worsens approximately by 0.10 R^2 in the case of the Captor 20001 O_3 sensor, and in

the case of the Captor NO sensor by 0.34 R^2 .

TABLE IV
AVERAGE CV R^2 FOR THE DIFFERENT SENSORS AND DUTY CYCLES,
WITH $T_{ref}=2\text{MIN}$.

Sensor	DC=1.00	DC=0.10	DC=0.03
20001 O_3	0.97	0.95	0.87
20001 NO_2	0.94	0.89	0.75
20001 NO	0.90	0.82	0.56
20002 O_3	0.97	0.94	0.84
20002 NO_2	0.92	0.88	0.74

In short, it is not necessary to have the node always powered on, a policy of sending the sensing subsystem to sleep and waking up the sensing subsystem has a minimal impact on data quality, and the power consumption can be reduced up to ten times.

VI. CONCLUSIONS

In this paper, we have studied the implications of the data gathering stage for an air pollution sensor node, both in terms of air quality and energy consumption. Most previous works, focus on the calibration of air pollution sensors, assuming that they have a high availability of measurements at a high sampling frequency. But, for real sensor network deployments with battery-powered IoT nodes mounting sensors, it is of vital importance to control the sampling rate, and the consequent duty cycle of the system, in order to minimize energy consumption. Therefore, we have built an experimental node called Captor with O_3 , NO_2 and NO sensors, which implements a high sampling rate, to investigate more efficient sensor data gathering strategies.

We have studied the impact of the sampling period of the sensing subsystem, and the number of samples taken in each period, on the sensor calibration using the best subset of sensors for calibration. Specifically, two strategies have been used, where in one the samples are measured uniformly during the sampling period, and another where the samples are taken consecutively. The results show that by taking few samples uniformly, regardless of the sampling period, the quality of the obtained calibration is good. In the case of sequential sampling as the sensing subsystem period increases the calibration gets worse, but with a period of about ten minutes and five or ten sequential samples the data quality is good. So, taking few uniform measures maintains the best data quality, and taking few consecutive samples works fine only for small periods (i.e., less than ten minutes). However, there is a problem with the uniform sampling strategy, and it is that when there exist a sensor response time to collect the sensor measurements the first strategy is no longer feasible because the node should be always on, being the second one the most effective and also feasible strategy. In addition, the results on the second strategy show that with a duty cycle about ten times lower than having the node always powered on, good data quality can be maintained, thus saving energy at little cost in terms of data quality. Finally, the results show that each sensor may require a different sampling rate.

REFERENCES

[1] G. Anastasi, M. Conti, M. Di Francesco, and A. Passarella, "Energy conservation in wireless sensor networks: A survey," *Ad hoc networks*, vol. 7, no. 3, pp. 537–568, 2009.

[2] E. Fassolo, M. Rossi, J. Widmer, and M. Zorzi, "In-network aggregation techniques for wireless sensor networks: a survey," *IEEE wireless communications*, vol. 14, no. 2, pp. 70–87, 2007.

[3] J. M. Barcelo-Ordinas, M. Doudou, J. Garcia-Vidal, and N. Badache, "Self-calibration methods for uncontrolled environments in sensor networks: A reference survey," *Ad Hoc Networks*, vol. 88, pp. 142–159, 2019.

[4] B. Maag, Z. Zhou, and L. Thiele, "A survey on sensor calibration in air pollution monitoring deployments," *IEEE Internet of Things Journal*, vol. 5, no. 6, pp. 4857–4870, Dec 2018.

[5] P. Ferrer-Cid, J. M. Barcelo-Ordinas, J. Garcia-Vidal, A. Ripoll, and M. Viana, "A comparative study of calibration methods for low-cost ozone sensors in iot platforms," *IEEE Internet of Things Journal*, vol. 6, no. 6, pp. 9563–9571, Dec 2019.

[6] L. Spinelle, M. Gerboles, M. G. Villani, M. Aleixandre, and F. Bonavita, "Field calibration of a cluster of low-cost available sensors for air quality monitoring. part a: Ozone and nitrogen dioxide," *Sensors and Actuators B: Chemical*, vol. 215, pp. 249–257, 2015.

[7] A. Bigi, M. Mueller, S. K. Grange, G. Ghermandi, and C. Hueglin, "Performance of no, no₂ low cost sensors and three calibration approaches within a real world application," *Atmospheric Measurement Techniques*, vol. 11, no. 6, pp. 3717–3735, 2018.

[8] Y. Wang, Y. Du, J. Wang, and T. Li, "Calibration of a low-cost pm2. 5 monitor using a random forest model," *Environment international*, vol. 133, p. 105161, 2019.

[9] L. Spinelle, M. Gerboles, M. G. Villani, M. Aleixandre, and F. Bonavita, "Field calibration of a cluster of low-cost commercially available sensors for air quality monitoring. part b: NO, CO and CO₂," *Sensors and Actuators B: Chemical*, vol. 238, pp. 706–715, 2017.

[10] P. Kumar, L. Morawska, C. Martani, G. Biskos, M. Neophytou, S. Di Sabatino, M. Bell, L. Norford, and R. Britter, "The rise of low-cost sensing for managing air pollution in cities," *Environment international*, vol. 75, pp. 199–205, 2015.

[11] A. Ripoll, M. Viana, M. Padrosa, X. Querol, A. Minutolo, K. M. Hou, J. M. Barcelo-Ordinas, and J. Garcia-Vidal, "Testing the performance of sensors for ozone pollution monitoring in a citizen science approach," *Science of the Total Environment*, vol. 651, pp. 1166–1179, 2019.

[12] M. A. Zaidan, N. H. Motlagh, P. L. Fung, D. Lu, H. Timonen, J. Kuula, J. V. Niemi, S. Tarkoma, T. Petäjä, M. Kulmala *et al.*, "Intelligent calibration and virtual sensing for integrated low-cost air quality sensors," *IEEE Sensors Journal*, vol. 20, no. 22, pp. 13 638–13 652, 2020.

[13] B. Mijling, Q. Jiang, D. d. Jonge, and S. Bocconi, "Field calibration of electrochemical no 2 sensors in a citizen science context," *Atmospheric Measurement Techniques*, vol. 11, no. 3, pp. 1297–1312, 2018.

[14] P. Nowack, L. Konstantinovskiy, H. Gardiner, and J. Cant, "Machine learning calibration of low-cost no 2 and pm 10 sensors: non-linear algorithms and their impact on site transferability," *Atmospheric Measurement Techniques*, vol. 14, no. 8, pp. 5637–5655, 2021.

[15] S. De Vito, E. Esposito, M. Salvato, O. Popoola, F. Formisano, R. Jones, and G. Di Francia, "Calibrating chemical multisensory devices for real world applications: An in-depth comparison of quantitative machine learning approaches," *Sensors and Actuators B: Chemical*, vol. 255, pp. 1191–1210, 2018.

[16] M. Si, Y. Xiong, S. Du, and K. Du, "Evaluation and calibration of a low-cost particle sensor in ambient conditions using machine-learning methods," *Atmospheric Measurement Techniques*, vol. 13, no. 4, pp. 1693–1707, 2020.

[17] M. I. Mead, O. Popoola, G. Stewart, P. Landshoff, M. Calleja, M. Hayes, J. Baldovi, M. McLeod, T. Hod gson, J. Dicks *et al.*, "The use of electrochemical sensors for monitoring urban air quality in low-cost, high-density networks," *Atmospheric Environment*, vol. 70, pp. 186–203, 2013.

[18] P. Han, H. Mei, D. Liu, N. Zeng, X. Tang, Y. Wang, and Y. Pan, "Calibrations of low-cost air pollution monitoring sensors for co, no₂, o₃, and so₂," *Sensors*, vol. 21, no. 1, p. 256, 2021.

[19] F. Karagulian, M. Barbiere, A. Kotsev, L. Spinelle, M. Gerboles, F. Lagler, N. Redon, S. Crunaire, and A. Borowiak, "Review of the performance of low-cost sensors for air quality monitoring," *Atmosphere*, vol. 10, no. 9, p. 506, 2019.

[20] A. Rebeiro-Hargrave, P. L. Fung, S. Varjonen, A. Huertas, S. Sillanpaa, K. Luoma, T. Hussein, T. Petäjä, H. Timonen, J. Limo *et al.*, "City wide participatory sensing of air quality," *Frontiers in Environmental Science*, p. 587.

[21] G. D. Astudillo, L. E. Garza-Castañon, and L. I. M. Avila, "Design and evaluation of a reliable low-cost atmospheric pollution station in urban environment," *IEEE Access*, vol. 8, pp. 51 129–51 144, 2020.

[22] D. E. Williams, "Low cost sensor networks: How do we know the data are reliable?" *ACS sensors*, vol. 4, no. 10, pp. 2558–2565, 2019.

[23] N. H. Motlagh, E. Lagerspetz, P. Nurmi, X. Li, S. Varjonen, J. Mineraud, M. Siekkinen, A. Rebeiro-Hargrave, T. Hussein, T. Petaja *et al.*, "Toward massive scale air quality monitoring," *IEEE Communications Magazine*, vol. 58, no. 2, pp. 54–59, 2020.

[24] E. Esposito, S. De Vito, M. Salvato, G. Fattoruso, and G. Di Francia, "Computational intelligence for smart air quality monitors calibration," in *International Conference on Computational Science and Its Applications*. Springer, 2017, pp. 443–454.

[25] N. Zimmerman, A. A. Presto, S. P. Kumar, J. Gu, A. Hauryliuk, E. S. Robinson, A. I. L. Robinson, and R. Subramanian, "A machine learning calibration model using random forests to improve sensor performance for lower-cost air quality monitoring," *Atmospheric Measurement Techniques*, vol. 11, no. 1, 2018.

[26] S. Munir, M. Mayfield, D. Coca, S. A. Jubb, and O. Osammor, "Analysing the performance of low-cost air quality sensors, their drivers, relative benefits and calibration in cities—a case study in sheffield," *Environmental monitoring and assessment*, vol. 191, no. 2, p. 94, 2019.

[27] E. S. Cross, L. R. Williams, D. K. Lewis, G. R. Magooon, T. B. Onasch, M. L. Kaminsky, D. R. Worsnop, and J. T. Jayne, "Use of electrochemical sensors for measurement of air pollution: correcting interference response and validating measurements," *Atmospheric Measurement Techniques*, vol. 10, no. 9, pp. 3575–3588, 2017.

[28] "Support circuits (ppb): Isb individual sensor board datasheet," [Online] <https://www.alphasense.com/products/support-circuits-air/>, [Accessed: 20 November 2021].

[29] "Alphasense ox-b431 sensor datasheet," [Online] <https://www.alphasense.com/products/ozone/>, [Accessed: 20 November 2021].

[30] "Alphasense no2-b43f sensor datasheet," [Online] <https://www.alphasense.com/products/nitrogen-dioxide/>, [Accessed: 20 November 2021].

[31] "Alphasense no-b4 sensor datasheet," [Online] <https://www.alphasense.com/products/nitric-oxide-safety/>, [Accessed: 20 November 2021].

[32] P. Ferrer-Cid, J. M. Barcelo-Ordinas, and J. Garcia-Vidal, "Raw data collected from no₂, o₃ and no air pollution electrochemical low-cost sensors," *In press*, 2021.

[33] S. Marathe, A. Nambi, M. Swaminathan, and R. Sutaria, "Currentsense: A novel approach for fault and drift detection in environmental iot sensors," in *Proceedings of the International Conference on Internet-of-Things Design and Implementation*, 2021, pp. 93–105.

[34] L. Sun, D. Westerdahl, and Z. Ning, "Development and evaluation of a novel and cost-effective approach for low-cost no₂ sensor drift correction," *Sensors*, vol. 17, no. 8, p. 1916, 2017.

[35] V. van Zest, F. B. Osei, A. Stein, and G. Hoek, "Calibration of low-cost no₂ sensors in an urban air quality network," *Atmospheric environment*, vol. 210, pp. 66–75, 2019.

[36] S. De Vito, E. Esposito, N. Castell, P. Schneider, and A. Bartonova, "On the robustness of field calibration for smart air quality monitors," *Sensors and Actuators B: Chemical*, vol. 310, p. 127869, 2020.

[37] P. Ferrer-Cid, J. M. Barcelo-Ordinas, J. Garcia-Vidal, A. Ripoll, and M. Viana, "Multi-sensor data fusion calibration in iot air pollution platforms," *IEEE Internet of Things Journal*, vol. 7, no. 4, pp. 3124–3132, 2020.